Robust image modeling technique with a bioluminesence image segmentation application

Article *in* Proceedings of SPIE - The International Society for Optical Engineering · February 2009

DOI: 10.1117/12.811491

3 authors, including:

Jianghong Zhong
Karolinska Institutet
17 PUBLICATIONS **108** CITATIONS
SEE PROFILE

Jie Tian
Chinese Academy of Sciences
661 PUBLICATIONS **7,114** CITATIONS
SEE PROFILE

Robust Image Modeling Technique with a Bioluminesence Image Segmentation Application

Jianghong Zhong[a,b], Ruiping Wang[a], Jie Tian[b]

[a]Department of Biomedical Engineering, School of Computer and Information Technology, Beijing Jiaotong University, Beijing 100044, China;
[b]Medical Image Processing Group, Key Laboratory of Complex Systems and Intelligence Science, Institute of Automation, Chinese Academy of Sciences, Beijing 100190, China

ABSTRACT

A robust pattern classifier algorithm for the variable symmetric plane model, where the driving noise is a mixture of a Gaussian and an outlier process, is developed. The veracity and high-speed performance of the pattern recognition algorithm is proved. Bioluminescence tomography (BLT) has recently gained wide acceptance in the field of in vivo small animal molecular imaging. So that it is very important for BLT to how to acquire the high-precision region of interest in a bioluminescence image (BLI) in order to decrease loss of the customers because of inaccuracy in quantitative analysis. An algorithm in the mode is developed to improve operation speed, which estimates parameters and original image intensity simultaneously from the noise corrupted image derived from the BLT optical hardware system. The focus pixel value is obtained from the symmetric plane according to a more realistic assumption for the noise sequence in the restored image. The size of neighborhood is adaptive and small. What's more, the classifier function is base on the statistic features. If the qualifications for the classifier are satisfied, the focus pixel intensity is setup as the largest value in the neighborhood.Otherwise, it will be zeros.Finally,pseudo-color is added up to the result of the bioluminescence segmented image. The whole process has been implemented in our 2D BLT optical system platform and the model is proved.

Keywords: robust image, classifier, segmentation, BLT, region of interest

1. INTRODUCTION

Imaging has become an indispensable tool in cancer research, clinical trials and medical practice. Imaging systems can be grouped by the spatial resolution that is attained into macroscopic, mesoscopic or microscopic systems. As one kind of macroscopic imaging systems, bioluminescence imaging[1,2] that does not only provide anatomical and physiological information, but also can obtain molecular information[3] is just emerging and adapted for `in vivo` analysis in clinical and preclinical use. The basis of optical imaging techniques is photons traveling through tissue and interacting with tissue components. The bioluminescence imaging signal depends on the expression levels of a luciferase enzyme, the presence of exogenously administered enzyme substrate (a luciferin), ATP, oxygen, depth and imaging time. In contrast to fluorescence techniques, there is no inherent background noise, which makes this technique highly sensitive[4] .

Consequently, the bioluminescence imaging is needed high performance digital systems designed for demanding low-light applications. The imaging system incorporates a wide selection of full frame, back-illuminated, scientific grade CCD, a choice of thermoelectric or cryogenic cooling, and low noise electronics to provide high sensitivity and high dynamic range. However, there are the unique requirements of low light near-infrared detection (NIR) in scientific imaging applications.An unfortunate drawback of back-illuminated CCD technology is that they exhibit `etaloning` - unwanted fringes caused by constructive and destructive interference patterns, which is dependent on several factors including spectral composition, degree of collimation and entrance angles of the illumination. Etaloning also can not be eliminated completely by deep depletion technology. Furthermore, the cosmic rays and defective pixels contribute to errors. In short, there are a list of pixels' gray values that

Further author information: (Send correspondence to Jie Tian)
Jie Tian: E-mail: tian@ieee.org, Telephone: 86-10-82618465, Fax: 86-10-62527995

Medical Imaging 2009: Biomedical Applications in Molecular, Structural, and Functional Imaging, edited by Xiaoping P. Hu, Anne V. Clough, Proc. of SPIE Vol. 7262, 72622H · © 2009 SPIE · CCC code: 1605-7422/09/$18 · doi: 10.1117/12.811491

are at least five times larger than the mean of the neighborhood and big standard deviations of the regions of interest which are more than 2.8, when the shutter of the imaging system is close during imaging.

That is why we need an effective model to remove noise and extract regions of interest while dealing with bioluminescence images in soft processing system. In the overwhelming majority of models based techniques for image processing tasks such as edge detection, image synthesis, image segmentation, etc., the image intensity array is assumed to be a multivariate Gaussian distribution. The Gaussian assumption is used primarily in estimating parameters of the image model fitted to the image. The corresponding estimation procedure is relatively easy. However, when the image contains impulse noise, the parameter estimates obtained from the Gaussian model do not appear to be appropriate. A more reasonable assumption for the noise sequence in the bioluminescence image is a contaminated Gaussian noise

$$\xi(i,j) = \begin{cases} w(i,j) & \text{with probability } 1-\beta \\ v(i.j) & \text{with probability } \beta \end{cases} \tag{1}$$

where $w(i,j)$ is a regular white Gaussian noise and $v(i,j)$ is an outlier process and the ratio of outlier β is assumed small (less than 5 percent).

Generally speaking, maximum likelihood or least squares estimators under the Gaussian assumption are very minor deviations from the Gaussian noise assumption. What it is a pity that mere a single outlier among 1000 observations can cause large error in the estimator. Therefore, robust estimators are needed in image models. According to Rangasami L.Kashyap'paper[5] , a robust estimator should possess the following property.

♢ It should have a reasonably good or optimal efficiency at the assumed noise distribution.

♢ It should be robust in the sense that the degradation in performance caused by a small number of outliers is relatively small.

♢ Somewhat larger deviation from the assumed distribution should not cause a catastrophe.

A large number of robust estimation algorithms have been published in the latest forty years, which can be classified into three main types of estimators: M-estimator, L-estimator, R-estimator. An M-estimator is a maximum likelihood-type estimator. An L-estimator is a linear combination of ordered statistics. An R-estimator is derived from the rank tests. At the same time, it is not difficult to extend M-estimators to the problem of image models, while other types of estimators are difficult to be used in problems other than location parameter estimation.

Although a robust procedure is necessary in most of the image processing applications, there are very few reports or articles published how to deal with BLI on the use of robust procedures. This article develops estimation algorithms for the nonsymmetric half-plane autoregressive image model and apply this robust method to the image restoration problem. Then, the BLI is segmented using the local expansion and statistics algorithm.

The core algorithm of the article is divided into two large parts. Restoration of an image in the presence of noise that is a fundamental problem in image segmentation is firstly described as detailed as possible. Kinds of image restoration methods based on the Gaussian noise assumption have been put forward. For example, Chellappa and Kashyap[6] made capital of a spatial interaction model to replace image intensity array and restored images with minimum mean square error criterion. M. Mattavelli et al[7] introduced a new image restoration method based on a 1-D Kalman filtering. Using the model of tuned channels, the corrupted image was decomposed into a set of perceptual components characterized by different orientations and frequencies. The restoration step was then performed on each component in one dimension following the appropriate orientation with the well-known Kalman algorithm. However, the impulsive component of the noise is only a small portion of the whole image, but it is not easy to be removed by the methods based on the Gaussian noise assumption because its amplitude is much higher than signal amplitude. Although nonlinear filtering measures such as median filter or α-trimmed mean filter are made use of to remove impulse noise , the edges are usually smeared and the result image after processing is blurred. Of cause, there is progress in the methods brought up to deal with the impulsive noise. For example, Li Deng and Ruihua Lu[8] proposed a blind image restoration method based on the genetic algorithm (GA) and the fuzzy control (FC) which consists in alternately estimating the PSF matrixes and image blocks by two kinds of GAs. Their experiment results were good. What a pity, the edge noise of

restored image can not be cleared completely, while the operation was complicated. We develop a restoration progressing based on the robust image model to deal with BLI real time. In our system BLI intensity array is represented by a nonsymmetric half-plane (NSHP) autoregressive model, and a robust parameter estimate and data cleaning algorithm is applied to restore images from impulse noise contamination.

Secondly, we develop an algorithm to segment the BLI. The goal of image segmentation is to partition the image plane into meaningful regions (where meaningful typically refers to a separation of regions corresponding to different objects in the image), as is well known. In the image segmentation field, traditional techniques do not completely meet the segmentation challenges mostly posed by bioluminescence images. Because the BLI gray value is usual less than ten units bigger than the background image gray level, and the variance of the region of interest in the BLI is at least 2.8. A lot of traditional methods come true in the MITK developed by our laboratory[9] , such as the Threshold Segmentation, the Region Grow Segmentation, the Interactive Segmentation, the Live Wire Segmentation, the Fast Marching Segmentation, and the LevelSet Segmentation. The outputs of these algorithms are not ideal for the BLI. However, the signal region can be withdrawn perfectly by the algorithm from the paper.

The Segmentation algorithm based on the robust image model introduced in the paper is a reasonable technique that is fit to BLT. It will make great progress in the inverse problem[10,11] because of more clear 2D surface images.

The rest of this paper is organized as follows. Section 2 presents the pretreatment of image restoration. In section 3, we give a introduction of the segmentation algorithm. The experiment results are shown in Section 4. Section 5 provides a summary of our work and talks about the future work.

2. ROBUST IMAGE RESTORATION

This section will describe the whole preprocessing using the robust image modeling technique for the following image segmentation. Although it is a mature technology, it is the first time to be used in BLI process. And we have a proved result.

2.1 Robust Parameter Estimation

First of all, the nonsymmetric half-plane model which behaves very much like one dimensional time series models must be introduced[5] . There is an assumption that the gray value of a BLI follows the nonsymmetric half-plane model. Let (i, j) be an index for the coordinate location, and $y(i, j)$ be the intensity at the coordinate (i, j). Let's define a nonsymmetric half-plane Ω as follow:

$$\Omega = \{(i,j) : (i = 0 \quad and \quad j < 0) \quad or \quad (i < 0 \quad and \quad j \in \forall)\} \tag{2}$$

where Ω is illustrated in Figure 1. The nonsymmetric half-plane members are indicated by X; $\bigodot$ is the origin.

Let s and p be indexes for two-dimensional coordinate locations. The useful property of Ω is: if $p \in \Omega$ and $s \in \Omega$ then $(s + p) \in \Omega$. An NSHP autoregressive model will be written as

$$y(s) = \sum_{r \in L} \theta_p y(s + p) + \alpha + \sigma\xi(s) \tag{3}$$

where the noise $\xi(\cdot)$ is zero mean, unit variance, and uncorrelated, while the neighbor set L is a subset of the nonsymmetric half-plane Ω. Equation (3) can be rewritten in the linear vector equation form

$$y(s) = \theta^T z(s) + \sigma\xi(s) \tag{4}$$

where θ is a parameter vector and $z(s)$ is a vector which consists of gray values of pixels in the neighbor set L and unit. The last element of the vector $z(s)$ is required to represent a constant gray level in the image

$$z(s) = [\{y(s + p), p \in L\}, 1]^T \tag{5}$$

The above model is used in our 2D real time BLI in vivo system.

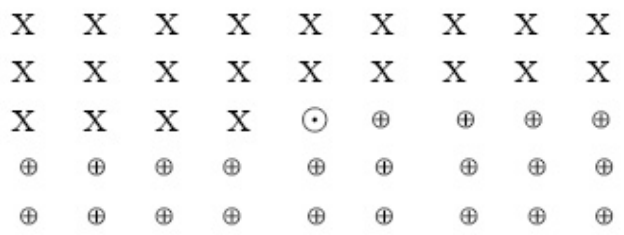

Figure 1. The nonsymmetric half-plane autoregressive model.

Now we should analyze the problem of the parameter estimation in the NSHP model. In the least squares estimation, we directly minimize the following function, with respect to θ:

$$\sum_{i,j}(y(i,j)-\theta^T z(i,j))^2 \tag{6}$$

The basic intention of a least squares estimation is to minimize the residuals. But the corresponding residual is very large and the least squares estimator is greatly influenced by this outlier, if one observation is an outlier. Consequently, the least squares estimator is not robust. To make sure the robustness of the estimator, we scale the residuals by a scale factor σ, which is noise intensity in the NSHP model (Equation 3). Then, we use a nonquadratic function ρ, which is a differentiable function possessing a bounded derivative, and it is symmetric about origin with $\rho(0)=0$.

Robust M-estimators are defined by the minimization of a nonquadratic function of normalized residuals. Let

$$Q(\theta,\sigma)=\frac{1}{mn}\sum_{i,j}[\rho(\frac{y(i,j)-\theta^T z(i,j)}{\sigma})+\frac{1}{2}]\sigma. \tag{7}$$

The residual should be normalized by the scale factor σ in the above criterion function because the M-estimator is not scale invariant. M-estimators are robust because the bounded function ρ limits the influence of outliers to a final estimator. Therefore, the M-estimators of NSHP autoregressive model are defined by the following minimization problem:

$$Minimize \quad Q(\theta,\sigma). \tag{8}$$

The M-estimator will also obtained by solving the following equations simultaneously:

$$\nabla_\theta Q(\theta,\sigma)=\frac{-1}{mn}\Sigma\psi(\frac{y(i,j)-\theta^T z(i,j)}{\sigma})z^T(i,j)=0 \tag{9}$$

$$\frac{\partial Q(\theta,\sigma)}{\partial\sigma}=\frac{1}{2}-\frac{1}{mn}\Sigma\chi(\frac{y(i,j)-\theta^T z(i,j)}{\sigma})=0 \tag{10}$$

where $\psi(x)=\partial\rho(x)/\partial x$ and $\chi(x)=x\psi(x)-\rho(x)$, and the function ψ is continuous and bounded.

Thus, there should be a reasonable choice of the ψ function not only for the robustness of estimator, but also for the fast convergence of the iterative procedure. The redescending ψ function yields higher efficiencies than the monotone ψ function for extremely heavy tailed distributions[12,13] . In our experiment and BLI system, a redescending ψ function is used as follows:

$$\psi(x)=\begin{cases} x, & |x|\le a \\ a\cdot sgn(x), & a<|x|\le b \\ \frac{c-|x|}{c-b}a\cdot sgn(x), & b<|x|\le c \\ 0, & |x|>c. \end{cases} \tag{11}$$

The robust estimator of the NSHP autoregressive model parameters defined in Equation (8) has many desirable properties, such as the asymptotic property which was proved by Nasburg and Kashyap[14] . However, the direct computation of the M-estimator is difficult, since it involves the minimization of a nonquadratic function of multiple parameters. Our system draws a lesson from the method introduced by R. L. Kashyap, and brings up a suitably iterative processing for BLI, of which some basically theoretical properties[5] were proved and shown in 1988. The minimization is done in the following way.

1) Let $\theta^{(0)}$ and $\sigma^{(0)}$ be initial estimates.

2) At the kth iteration, we have $\theta^{(k)}$ and $\sigma^{(k)}$. Compute the residual $r^{(k)}$

$$r^{(k)}(i,j) = y(i,j) - {\theta^{(k)}}^T z(i,j), \tag{12}$$

where $z(i,j)$ is defined in Equation (5). Compute the censored residual $\hat{r}^{(k)}$

$$\hat{r}^{(k)}(i,j) = \psi(\frac{r^{(k)}(i,j)}{\theta^{(k)}})\theta^{(k)}. \tag{13}$$

3) Compute $\theta^{(k+1)}$ and $\sigma^{(k+1)}$ as follows:

$$\theta^{(k+1)} = \theta^{(k)} + \tau^{(k)}, \tag{14}$$

where

$$\tau^{(k)} = [\sum_{i,j} z(i,j)z^T(i,j)]^{-1}[\sum_{i,j} z(i,j)\hat{r}^{(k)}(i,j)], \tag{15}$$

$${\sigma^{(k+1)}}^2 = \frac{1}{mn}\sum_{i,j}[\hat{r}^{(k)}(i,j)]^2. \tag{16}$$

4) Repeat steps 2)$\longrightarrow$3) until the differences $\eta_1 = \|\theta^{(k+1)} - \theta^{(k)}\|$ and $\eta_2 = \|\sigma^{(k+1)} - \sigma^{(k)}\|$ become less than $\eta_i^{(0)} \quad (i = 1, 2)$.

2.2 Image Restoration

Now we give a list of steps during image restoration with noise images according the above theoretical model. First and foremost, we have some simulation experiments using a BLI corrupted by a white Gaussian (0,1) noise sequence to assess the mean square error of the robust parameter estimator and derive the initial parameters performing best, such as $\theta^{(0)}$, $\sigma^{(0)}$ and the size of the neighbor set L. Under the guidance of the robust parameter estimation algorithm, the values of

$$\frac{1}{N}\sum_i(\theta_i^{(k)} - \theta_i^{(0)})^2$$

are less than 0.008 with different β values, while N is the number of tested images. And we find out the following set of initial parameters is practicable:

$$L = \{(0,-1),(-1,0),(-1,-1)\}, \quad {\theta^{(0)}}^T = [0.3, 0.3, 0.3], \quad \sigma^{(0)} = 0.5, \quad and \quad \eta_i^{(0)} = 0.001, i = 1, 2.$$

Secondly, we make C++ program to carry out the iterative processing with the input of the above set of initial parameters. Happily, the algorithm is worthy of being adopted. Finally, our BLI system,named WinMI, absorbs this kind of preprocessing.

However, it should be noted that both the photographic image and the correspondingly luminescence image need to be restored while the overlap image should come out in the BLI system. Because the ultimate goal of the whole processing is to obtain the region of interest, but there are some tiny geometry offsets between the crude image and the restored image. And we need the photographic image to mark the spatial location of bioluminescence information distribution.

3. ROBUST IMAGE SEGMENTATION

Image segmentation based on robust modeling technique should be narrated in the section in detail. Our sole motive is to the most effectively display the bioluminescence regions in a image by the method of image segmentation.

The aforementioned pretreatment is only some a removal of overall noise. In general, the BLI[15] is originated in the live mice in a darkroom without any external light. The maximum of the intensities in the BLI is less then 0.25 percent in comparison with the max gray level 65535 while the exposure time is 1 second using the our BLI in vivo system with a VersArray Camera and the binning numbers are 1. What is more, the intensities of the corresponding background image and BLI are in the same range. The differences between them is no more than 30 gray levels, generally speaking. What a pity, there are a number of small spots scattering in the BLI because of the extremely strong light sensitivity in the image system in vivo. Those are usually not the bioluminescence information and need to be removed. After carefully analyzing it with the image feature, we could find out suitable processing algorithms. Most likely to think of a solution to the problem is to use the software the Roper Scientific company developed, named WinView32. It is well known that there are many other sophisticated algorithms in the 3DMed platform developed by our lab. But the results by the above-mentioned algorithms are not ideal and the computing speed is very low.

Therefore, there is an urgent need for a high-speed efficient segmentation algorithm. Although there has been significant interest in graph-based approaches to medical image segmentation in the past few years[16,17] , So few published articles about BLI segmentation can be referred. To this purpose, we propose a new approach which is the local expansion and statistics algorithm. The core of the algorithm is that every pixel value is reassigned in the light of neighborhood expansion algorithms filter when it is in a special statistics range of intensities in the neighborhood. If the center pixel value does not satisfy such a condition, it is set zero. Detailed steps are described below.

1) Initialization of matrix mode. The matrix mode $\Gamma^{(i,j)}$ is filled full with pixels intensities coming from the uniform neighborhood of the center pixel $f(i,j)$, where f means the original gray image matrix and $M \in Z, N \in Z, k \in Z, Z$ represents the positive integer set.

$$\Gamma^{(i,j)}[m,n] = f(i-k+m-1, j-k+n-1) \tag{17}$$

$$[M,N] = size(f), \quad 1 \le i \le M, 1 \le j \le N \tag{18}$$

$$size(\Gamma^{(i,j)}) = [2k+1, 2k+1], \quad 1 \le m \le 2k+1, 1 \le n \le 2k+1 \tag{19}$$

2) Re-distribution of center pixel value. It should be the implementation of statistics and analysis calculating process for $\Gamma^{(i,j)}$ as the input variable, where T is the gray level threshold and Υ is the local statistics threshold number.

$$\begin{gathered} num = 0 \\ while(\Gamma^{(i,j)}[m,n] \ge T) \\ \{num = num + 1\} \end{gathered} \tag{20}$$

$$f(i,j) = \begin{cases} max(\Gamma^{(i,j)}) & num \ge \Upsilon \\ 0 & num < \Upsilon \end{cases} \tag{21}$$

3) Pseudo-color processing in the segmented image. It changes the gray image $f(i,j)$ into the RGB color image, where R is the red channel of the data matrix of the pseudo-color image $g(i,j)$ and G is the green channel while B indicating the blue channel.

$$g(i,j) = \{R, G, B\} \tag{22}$$

$$R(i,j) = f(i,j) - min(f(i,j)) \tag{23}$$

$$G(i,j) = 1.5 \times \sqrt{(max(f(i,j)) - g(i,j)) \times (g(i,j) - min(g(i,j)))} \tag{24}$$

$$B(i,j) = max(f(i,j)) - f(i,j) \tag{25}$$

In the BLI system in vivo, we proved these initial parameters which perform best: $k = 2$,$T = 1000$, $\Upsilon = 8$.

4. EXPERIMENTAL RESULTS

The BLI system in vivo , named WinMI, developed by ourselves comes true. And the robust image modeling technique has proved. The section will describe a whole set of processes in the next paragraph.

First of all, we collect a photographic image , a background image, and a bioluminescent image using the BLI system in vivo with the help of WinMI software system. The images to be processed should be minus the background image, which are shown in Figure 2. The photographic image is a grayscale image with a short

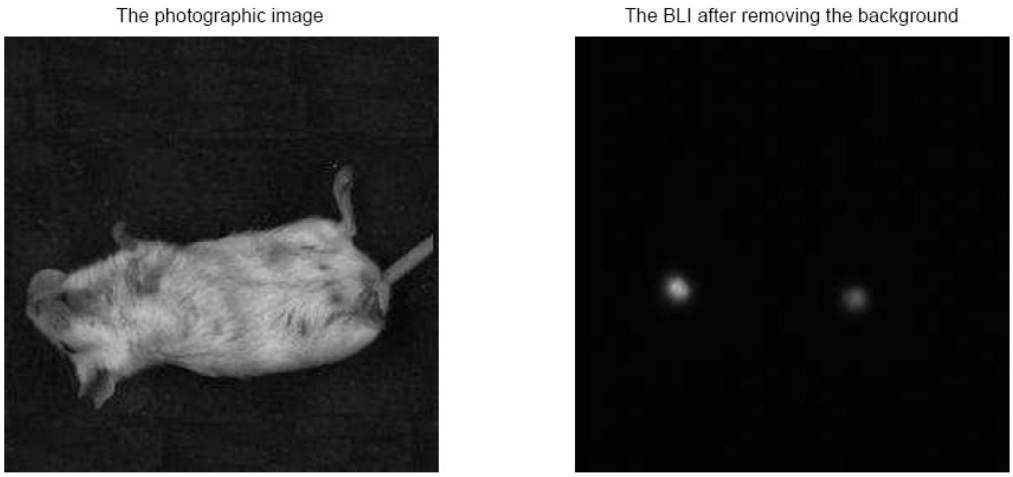

Figure 2. The original images.

exposure of the mouse illuminated by the lights located at the top of the imaging chamber. The BLI is one with a longer exposure of the mouse taken in darkness to capture low luminescence emission. And the background image is collected while the shutter is close, which should be subtracted to remove the influences from readout noise and dark current, etc.

Next, we draw a comparison between the images and the restored images. In Figure 3, we can find out that the contrast is stronger and the details show more clearly by observing (b) in comparison with (a). The same situation occurs in Figure 4.

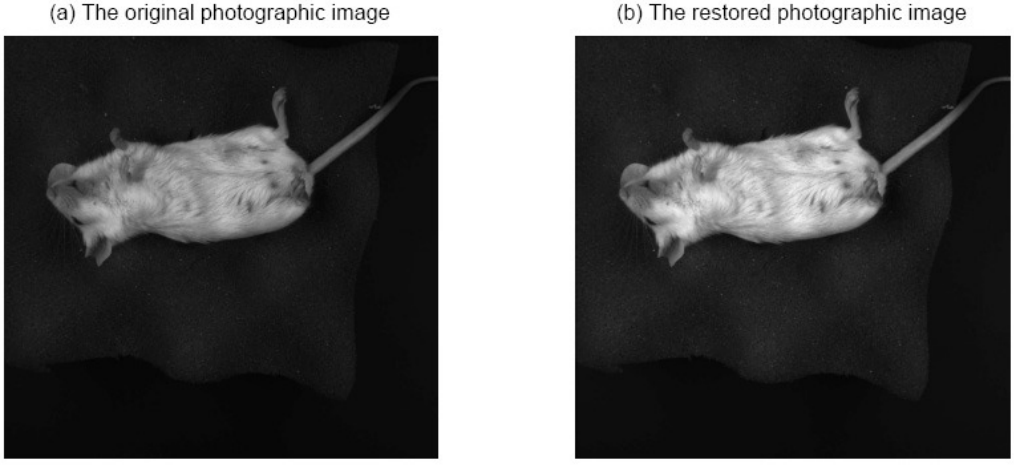

Figure 3. The comparison drawn from photographic images.

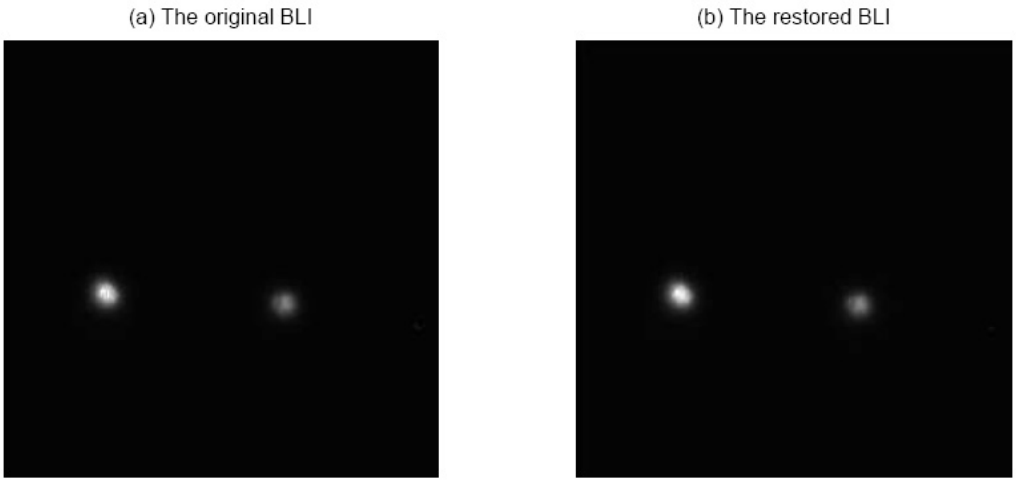

Figure 4. The comparison drawn from bioluminescent images.

In order to show clearly the improved image after robust image restoration, Table 1 is made. The standard deviation of the values in a image is one of important evaluation parameters while differences are significant. The restored images have low standard deviations. In Table 1, `photographic` represents the photographic images and `bioluminescent` indicates the bioluminescence images. All of them contain the crude image and the restored image.

Table 1. The comparison of robustly restored images and original images through the standard deviation of the values .

Restored Image	$\frac{std2(OriginalImage)-std2(RestoredImage)}{std2(OriginalImage)}$
photographic	10.05/100
bioluminescent	10.43/100

Finally, the paper displays the results of two typical image segmentation algorithms.

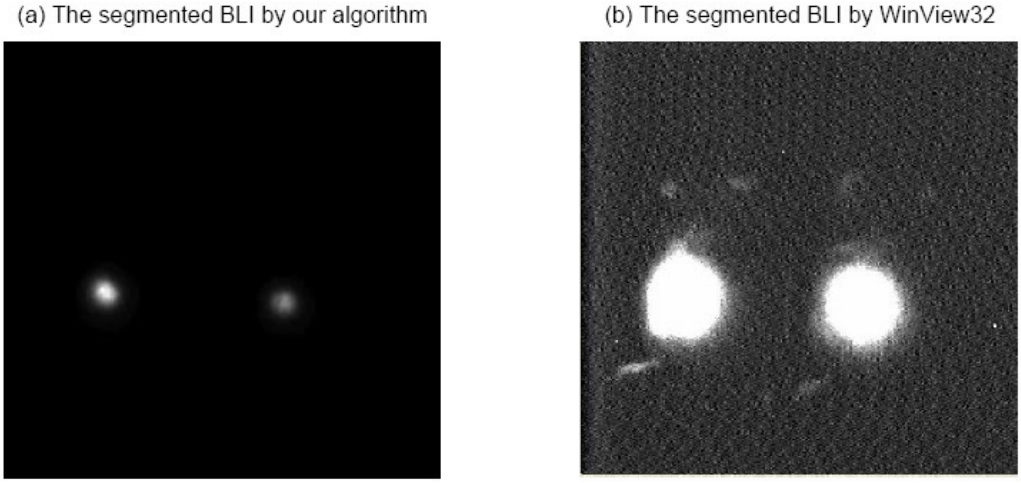

Figure 5. The different segmented results.

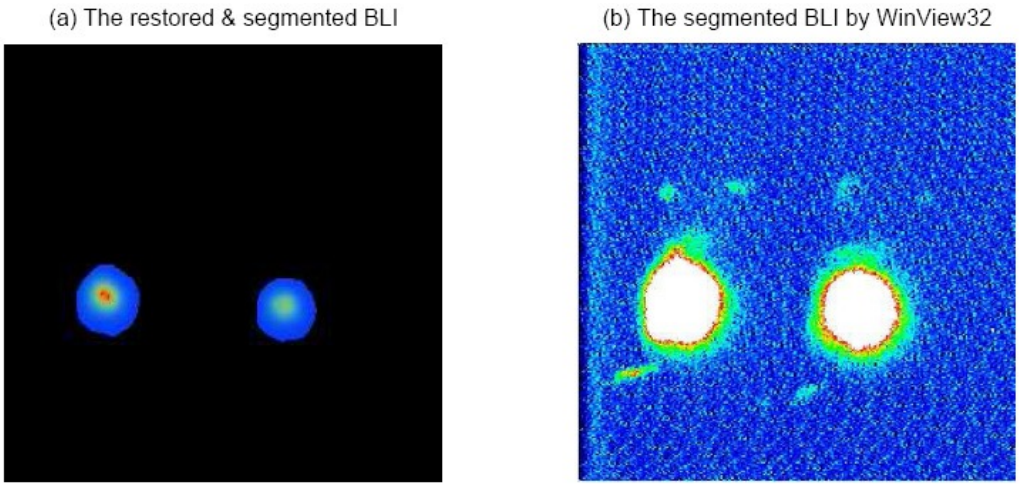

Figure 6. The different segmented results.

In Figure 5 , (a) is the result coming from our robust model while (b) is the output of WinView32 which is a software with the purchase of machine equipment from Roper Scientific, Inc. There is only one non-zero region in Figure 5.(a), which is in line with the objective fact that there is only a light source in the live mouse because of tumor cell transplantation in some a region in vivo. Then, we change the grayscale images into the pseudo-color ones displayed in Figure 6. It better shows the superiority of our algorithm.

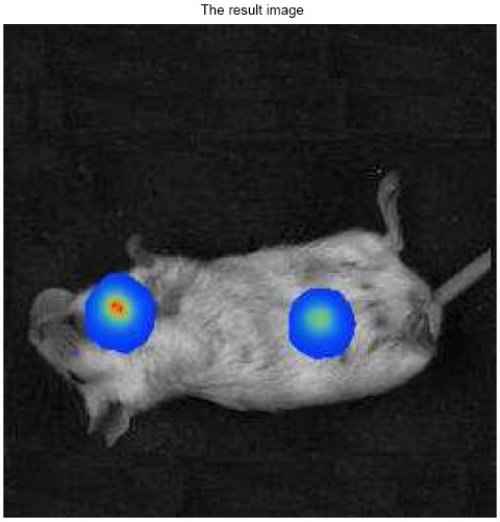

Figure 7. The result image.

At the end of the experimental phase, the output image which we look forward to is obtained as shown in Figure 7. The size of images is 256×256 . Every step of the above-mentioned can be completed in less than one second with a ThinkCentre computer from Lenovo, Inc.

5. CONCLUSIONS

The robust image model technique can offer an approach which can fast and correctly segment the BLI while restoring the image with the unknown noise. The developed model has been applied in our in vivo small animal

molecular imaging system, and can accurately determine the photons of every pixel in the region of interest. The future work will focus on the self-adaptive BLI segmentation in the above model.

ACKNOWLEDGMENTS

This paper is supported by the Project for the National Basic Research Program of China (973) under Grant No.2006CB705700, Changjiang Scholars and Innovative Research Team in University under Grant No.IRT0645, CAS Hundred Talents Program, CAS scientific research equipment develop program (YZ0642,YZ200766),863 program under Grant No. 2006AA04Z216, the Joint Research Fund for Overseas Chinese Young Scholars under Grant No.30528027, the National Natural Science Foundation of China under Grant No. 30672690, 30600151, 30500131, 60532050, 60621001, Beijing Natural Science Fund under Grant No. 4071003.

REFERENCES

1. G. Wang, W. Cong, and et al, "Overview of bioluminescence tomography–new molecular imaging modality," *To appear in Frontiers in Bioscience* , 2007.
2. W. Han and G. Wang, "Bioluminescence tomography: Biomedical background, mathematical theory, and numerical approximation," *Journal of Computational Mathematics* **26**, pp. 324–335, 2008.
3. N. Craft, K. W. Bruhn, B. D. Nguyen, A. De, and et al, "Bioluminescent imaging of melanoma in live mice," *Journal of Investigative Dermatology* **125**, pp. 159–165, 2005.
4. R. Weissleder and M. J. Pittet, "Imaging in the era of molecular oncology," *Nature* **452**, pp. 580–589, 2008.
5. R. L. Kashyap and K.-B. Eom, "Robust image modeling techniques with an image restoration application," in *IEEE Trans and Acoust, Speech, Signal Processing* **36**, pp. 1313–1325, 1988.
6. R. Chellappa and R. L. Kashyap, "Digital image restoration using spatial interaction models," in *IEEE Trans and Acoust., Speech, Signal Processing.* **ASSP-30**, pp. 461–472, 1982.
7. M. Mattavelli, G. Thonet, V. Vaerman, and B. Macq, "Image restoration by 1-d kalman filtering on oriented image decompositions," in *Acoustics, Speech, and Signal Processing, ICASSP-96. IEEE International Conference on*, **4**, pp. 2271 – 2274, 1996.
8. L. Deng and R. Lu, "A blind image restoration method based on the genetic algorithm and the fuzzy control," in *Audio, Language and Image Processing, ICALIP 2008. International Conference on*, pp. 330–334, 2008.
9. J. Tian, J. Xue, and Y. Dai, *Development and Implementation of Medical Imaging Algorithm Toolkit*, Tsinghua University Press, Beijing, 2007.
10. W. Cong, G. Wang, A. Cong, and et al, "Practical reconstruction method for bioluminescence tomography," *Optics Express* **13 No.18**, pp. 6756–6771, 2005.
11. J. Feng, J. Tian, and et al, "An optimal permissible source region strategy for multispectral bioluminescence tomography," *Optics Express* **16 No.20**, pp. 15640–15654, 2008.
12. P. J. Huber, *Robust Statistics*, Wiley, New York, 1981.
13. W. J. J. Rey, *Introduction to Robust and Quasi-Robust Statistical Methods*, Springer-Verlag, New York, 1983.
14. R. E. Nasburg and R. L. Kashyap, "Robust parameter estimation in dynamic systems," in *Proceedings of the 1975 Conference on Information Sciences and Systems*, pp. 370–375, The Johns Hopkins University, Baltimore, Maryland 21218, 1975.
15. J. Tian, J. Bai, X. Yan, S. Bao, Y. Li, W. Liang, and X. Y. et al, "Multimodality molecular imaging," *IEEE Engineering in Medicine and Biology Magazine* **27 No.5**, pp. 48–57, 2008.
16. S. Wang and J. M. Siskind, "Image segmentation with ratio cut," *Pattern Analysis and Machine Intelligence, IEEE Transactions on* **25**, pp. 675–690, 2003.
17. L. Zhang and Q. Ji, "Integration of multiple contextual information for image segmentation using a bayesian network," in *Computer Vision and Pattern Recognition Workshops, CVPR Workshops 2008. IEEE Computer Society Conference on*, pp. 1–6, 2008.